Studies of the orthoamphiboles. IV. Mössbauer spectra of anthophyllites and gedrites

ANTHONY D. LAW*

Department of Earth Sciences, University of Oxford, Parks Road, Oxford OX1 3PR

Abstract

Fitted Mössbauer spectra are presented for a set of anthophyllites and gedrites. Despite their complexity it is possible to obtain fits for gedrite spectra and the Mössbauer parameters are consistent with results for anthophyllites from this and previous studies. At least three doublets are required to fit the Fe^{2+} absorption in gedrites; there is no single model at present to explain the behaviour of the spectra. Fe^{3+} absorption is also resolved.

KEYWORDS: orthoamphiboles, Mössbauer spectra, anthophyllites, gedrites.

Introduction

MÖSSBAUER spectroscopic studies of of the orthoamphiboles, anthophyllite and gedrite, are of value because of the direct evidence which Mössbauer data provide of the distribution of iron species in the structure. This in turn helps to unravel the many mineralogical problems associated with these minerals (e.g. Spear, 1980; Seifert and Virgo, 1974; Hawthorne, 1983a, 1988).

Seifert (1977) reported Mössbauer spectra of a series of anthophyllites and established a relationship between both doublet centre shifts and line half-widths, and the Al content of the mineral. He inferred from these trends that the problems of fitting gedrite spectra would present 'serious or possibly even insurmountable difficulties' because of the likely close overlap of the peaks. He also presented, but without any attempt at fitting, a spectrum of the Orange area gedrite I34I (Robinson and Jaffe, 1969).

This paper reports, with at this stage only limited interpretation, the results of fitting Mössbauer spectra of both anthophyllites and gedrites. Although the difficulties anticipated by Seifert (1977) are amply confirmed, the peak parameters which are obtained are consistent with the trends established from anthophyllite spectra. This gives confidence that the results can be interpreted to give useful and credible mineralogical information.

* Present address: BP Exploration Company Ltd., Britannic House, Moor Lane, London EC2Y 9BU.

Specimens

Mössbauer spectra have been determined for most of the anthophyllites of Law (1981) and the gedrites of Law (1982). The suite includes two amphiboles for which site occupanies have been determined by X-ray investigation: the Dillon anthophyllite (Finger, 1969) and the Orange area gedrite I34I (Papike and Ross, 1970; Robinson and Jaffe, 1969). Gedrite 003 is the '36 percent iron anthophyllite' and anthophyllite 002 the '23 percent iron anthophyllite' of the early report by Bancroft et al. (1969). The specimens' previously reported provenance and analyses are summarized in Table 1 and their compositions are plotted in Fe^{2+}–Mg–Al composition space (i.e. ignoring Na and Fe^{3+}) in Fig. 1.

Seifert (1977) has given new analyses for the Dillon anthophyllite 015, no. 30 of Rabbit (1948); for the St. Prejet anthophyllite 013 (Fabries and Perseil, 1971); and for an anthophyllite from Kongsberg, Norway, the same area as my 002. For new results presented here, the original published analyses are used.

Experimental

512-channel spectra described here were determined using the Nuclear Instruments spectrometer described by Burns and Greaves (1971), except for the 256-channel spectrum of the Kitakami ferrogedrite (specimen 009) which was determined in 256 channels using the Austin Associates spectrometer described by Burns (1972). Typical
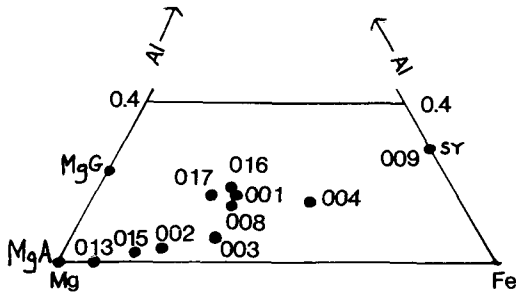
FIG. 1. Composition of specimens in (Mg–Fe^{2+}–Al^{vi}) space. Also included are end-member Mg–anthophyllite, Mg$_7$Si$_8$O$_{22}$(OH)$_2$ (MgA); and Mg–gedrite, Na$_{0.5}$Mg$_{5.5}$Al$_{1.5}$·Si$_6$Al$_2$O$_{22}$(OH)$_2$ (MgG). These and the Kitakami ferrogedrite (009) give an indication of the limits of the anthophyllite–gedrite compositional space.

baseline count rates were from 5×10^5 to 2×10^6.

Spectra were determined at ambient temperature and, for some specimens, at liquid nitrogen temperature using the techniques and cryostat described by Burns and Greaves (1971). A nominal temperature of 80 K will be quoted for the latter.

Computer fitting

Spectra were fitted using versions of the classic program by Stone (1967), run on ICL 1900 and CDC 7600 computers. Pure Lorentzian lineshapes were used throughout. The use of other profiles such as the Voigt or Gaussian-broadened Lorentzian profile (Evans and Black, 1970) has been discussed by a number of authors (e.g. Dollase and Gustafson, 1982). However, spectra of anthophyllites were satisfactorily fitted by Lorentzians and there could be no statistical justification for using the more complex profile (cf. Law, 1973). Many gedrite spectra cannot be satisfactorily fitted, but the resolution of peaks in these spectra is not sufficient to allow statistical tests to differentiate between different lineshapes. It would be impossible to separate the effects of lineshape from other much greater effects.

Particularly in complex spectra of gedrites, it was necessary to constrain fits. Constraints simplify the model being tested by fitting, reducing the number of parameters being estimated (cf. Hawthorne, 1983a, 1988). Most typically, the widths and, sometimes, areas of the components of doublets were constrained equal. Where parameters are fitted without constraints, their correlation coefficients provide further evidence to

support the model (or otherwise!). For example, the areas and widths of a pair of peaks which are components of the same doublet would be expected to show a strong positive correlation. Conversely, where two peaks overlap strongly their parameters often shown a strong negative correlation which indicates that the fitting process cannot resolve them effectively.

Some of the problems of distinguishing between different fits have been discussed by Law (1973), and reviewed by Hawthorne (1983a, 1988); they are implicit also in this paper although not explicitly discussed.

Calibration and recalculation

To calibrate the spectrometer, spectra of natural iron foil (the inner four peaks, at the normal spectrometer settings) were obtained and computer fitted in the normal way. The resulting line positions and estimated errors were refined against the standard iron foil peak velocities and standard errors from Stevens and Preston (1970) to fit a straight line, with errors estimated for slope and intercept. The program (Law, unpublished) takes account of errors in both x and y coordinates. The parameters of the fitted line (slope and intercept) and their estimated errors are the calibration constants used to calculate peak velocities. Estimating error is taken into account at all stages. Parameter covariances contribute to the estimated errors in the Mössbauer doublet parameters centre shift (CS or δ), quadruple splitting (QS or Δ), mean linewidth (Γ), and relative area (A); see Appendix.

There is no evidence (e.g. from spectra at different temperatures) that the absorptions giving rise to different doublets have different recoil-free fractions. Peak area ratios are, therefore, assumed to be directly proportional to the ratios of iron species giving rise to the absorption.

Results—anthophyllites

Results for anthophyllites are summarized in Table 2. Anthophyllite spectra were fitted to two doublets for Fe^{2+}, which are lettered A (outer) and C (inner). Peak C of this study corresponds to B of Seifert (1977); B is used to denote a third Fe^{2+} doublet fitted between the other two in some spectra. A doublet for Fe^{3+} is denoted F. Where it is necessary to distinguish between the low- and high-velocity components of a doublet, these are denoted 1 and 2 respectively. Results from Seifert (1977) for the same specimens are included in tables and diagrams for comparison.

Dillon anthophyllite (015). The spectrum (Fig.

Table 1a. Compositions of specimens

	K	Na	Ca	Mg	Fe^{2+}	Fe^{3+}	Mn	Ti	Al^{vi}	Si	Al^{iv}	OH	Σ(vi)	Σ(iv)
Anthophyllites														
015	0.07	0.01	0.09	5.48	1.28	0.00	0.01	0.00	0.15	7.84	0.16	1.89	7.09	8
002	–	–	0.17	5.00	1.61	0.04	0.07	–	0.20	7.86	0.14	1.71	7.09	8
013	0.00	0.00	0.16	6.25	0.65	0.19	0.01	0.01	0.00	7.58	0.41	1.74	7.27	7.99
003	0.00	0.21	0.13	3.94	2.21	0.10	0.07	0.02	0.42	7.19	0.81	2.22	7.10	8
Gedrites														
001	–	–	0.08	3.44	2.35	–	–	–	1.15	6.79	1.21	(2)	7.02	8
004	–	–	0.08	2.44	3.41	–	–	–	1.15	6.67	1.33	(2)	7.08	8
008	0.03	0.34	0.09	3.27	2.18	0.10	0.04	–	1.00	6.51	1.49	2.65	7.05	8
016	0.01	0.54	0.04	2.97	2.32	0.13	0.03	0.03	1.23	5.87	2.13	2.58	7.30	8
017	–	0.41	0.07	3.55	1.89	0.26	0.04	0.05	0.98	6.38	1.62	2.01	7.27	8
009	0.36	0.01	0.01	0.01	4.48	0.27	0.31	0.06	1.87	6.15	1.85	1.93	7.38	8

Notes

001,004: microprobe analyses, total Fe recalculated as Fe^{2+}. No K, Na analysis.
003: Cl 0.00, F absent
016: Li 0.02, Cr 0.00, P 0.00, Cl 0.00, F 0.00
017: Li 0.02, P 0.00, Cl 0.00, F 0.04

Table 1b. Origins of specimens

015: Dillon complex, Beaverhead & Madison counties, Montana, USA. USNM 117227; Rabbitt (1948) no. 30.

002: Kongsberg, Norway; Iskyul (1925). From Dr R G Burns.

013: St. Prejet, Haute-Loire, France; American Museum of Natural History, AMNH 18894. Studied by Fabries & Persell (1971), donated by Dr Fabries.

003: Bancroft, Ontario, Canada; Tilley (1957). From Dr R G Burns.

001: Bamle (or Bamble), Telemark, Norway; des Cloizeaux (1877); Pisani (1877); Kunitz (1930); Rabbitt (1948) no. 19 [not no. 18 as given erroneously by Rabbitt]. Analysis by Kunitz; specimen through Dr Burns.

004: Kuurila, Kalvola, Finland; Eskola (1936); Rabbitt (1948) no. 2 may be similar. Microprobe analysis (1969). From Helsinki Yliopisto Kivi-museo.

008: Bullsbrook, Western Australia; Simpson (1931); Rabbitt (1948) no. 7. British Museum (Natural History), BM 1932,1088.

016: Orange area, Massachussetts, USA; Robinson & Jaffe (1969) no. 134I. No. 002 of Papike & Ross (1970). From Dr Robinson.

017: as 016; Robinson & Jaffe (1969) no. 134JX. From Dr. Robinson.

009: Kitakami mountainland, NE Japan; Seki & Yamasaki (1957). From Dr. Seki.

2a) is typical of anthophyllites and comprises two Fe^{2+} absorptions which are assigned to Fe^{2+} in M4 (the inner, more intense, doublet C) and in $M1 + M2 + M3$ (the outer doublet A). The area ratio agrees reasonably with the site occupancies from structural refinement (Finger, 1969, based on a partial chemical analysis) and with the previously reported Mössbauer result (Seifert, 1977). Dyar (1984) has commented on the extent of comparability between results obtained from different Mössbauer laboratories.

Correlation coefficients between the linewidths and areas of the two fitted doublets (around −0.3) and between the areas and widths of the components of each doublet (around +0.7) indicate that although, for this spectrum, the residual of 553 for the 512 channel spectrum is statistically accep-table and the centre shift, quadruple splitting and linewidth values are all reasonable for silicates, the spectrum is not fully resolved in the four peak fit. This is in line with the interpretation that the A peak corresponds to closely overlapping absorptions from Fe^{2+} at $M1$, $M2$ and $M3$.

Other spectra of this anthophyllite gave high residuals (over 700) when fitted to four peaks. It was possible to fit an additional doublet (B), reducing the residual in these cases to a statistically acceptable value. One such fit is included in Table 2. It is instructive to consider it to see the behaviour of the fitting process. The B peaks in the six peak fit have taken their intensity from the C peaks (assumed to represent iron at $M4$ only) of the four peak fit. They are highly correlated with the remaining C peaks. This is typical

Table 2. Mössbauer peak parameters for anthophyllites

	Temp		δ	Δ	Γ	A	ΔA
015	A	A	1.121(8)	2.83(2)	0.33(2)	0.148(7)	<+0.001
		C	1.102(6)	1.89(1)	0.309(3)	0.852(9)	~0.04
015s	A	A	1.155	2.740	0.30	0.084	+0.002
		C	1.134	1.836	0.32	0.916	-0.066
002	A	A	1.121(8)	2.75(2)	0.34(3)	0.18(1)	+0.01
(562)		C	1.113(4)	1.877(9)	0.313(5)	0.82(2)	-0.03
002s	A	A	1.146	2.704	0.36	0.159	+0.001
		C	1.131	1.848	0.30	0.841	-0.045
002	80	A	1.263(6)	3.11(1)	0.307(4)	0.129(5)	–
(529)		B	1.299(9)	2.45(2)	same	0.087(6)	–
		C	1.239(2)	1.919(5)	same	0.078(1)	–
002s	80	A	1.263	2.964	0.42	0.143	+0.005
		C	1.258	1.901	0.31	0.857	-0.043
013	A	A	1.115(3)	2.851(7)	0.230(10)	.101(4)	-0.01
		C	1.135(1)	1.889(2)	0.272(2)	0.899(6)	-0.13
013s	A	A	1.153	2.783	0.27	0.078	-0.004
		C	1.131	1.834	0.29	0.922	-0.038
003	A	A	1.146(4)	2.86(2)	0.23(2)	0.16(3)	–
(587)		B	1.166(4)	2.47(3)	0.39(4)	0.28(6)	–
		C	1.120(3)	1.87(1)	0.344(7)	0.57(2)	–
003	80	A	1.258(3)	3.12(1)	0.28(2)	0.17(3)	–
(598)		B	1.276(4)	2.59(2)	0.49(6)	0.33(6)	–
		C	1.240(2)	1.901(5)	0.301(7)	0.48(2)	–
		F	0.57(2)	0.83(4)	0.27(7)	0.024(5)	–

Six peak fit for Dillon anthophyllite (see text):

			δ	Δ	Γ	A	ΔA
015	A	A	1.135(5)	2.81(1)	0.35(2)	0.174(9)	-0.011
(587)		B	1.155(6)	2.00(2)	0.30(1)	0.40(6)	-0.17
		C	1.141(3)	1.78(1)	0.264(8)	0.43(6)	+0.12

Notes
δ, Δ and Γ (mean linewidth) in mm/sec relative to iron foil (see text), estimated errors in parentheses in units of last decimal place. Areas normalised. ΔA is asymmetry [difference between component areas as A(high)~A(low)]: where a dash appears, component areas were constrained equal.

's' denotes results from Seifert (1977), notation changed in line with convention adopted here; published estimated error for these δ and Δ values is ±0.005 mm/sec. Value in parentheses under specimen number in first column is residual ('chi-squared'); see Law (1973).

Temperature: 'A' in second column denotes ambient temperature, '80' denotes liquid nitrogen cooling (see text)

of many attempts to fit a third Fe^{2+} doublet in orthoamphibole spectra.

Kongsberg anthophyllite (002). A two-doublet fit to the spectrum of this anthophyllite gave results consistent with the lower-resolution study by Bancroft *et al.* (1966). Two doublet fits to spectra of this anthophyllite tended to give high residuals, but additional peaks were difficult to fit. The spectrum is similar in appearance to that of the Dillon anthophyllite.

A spectrum determined at 80 K (Fig. 2b) was fitted to 6 peaks. The CS, QS and linewidth values are comparable to results at this temperature for other silicates, and to those obtained by Seifert (1977) for his Kongsberg specimen. For this fit, the linewidths of all peaks were constrained equal and the areas of components of each doublet were

constrained equal. Thus the fitted model represents a spectrum in which each peak is from Fe^{2+} at a single site, or at sites of very similar symmetry. The extra doublet (B) is fitted roughly midway between A and C, and area ratios suggest that A represents Fe^{2+} at three of the ($M1$, $M2$, $M3$) sites and B the other two.

St. Prejet anthophyllite (013). Results from a four peak fit are similar to those for the Dillon anthophyllite and to those for the same specimen from Seifert (1977).

Bancroft anthophyllite (003). This amphibole has more aluminium and iron, and less Mg, than the Dillon, Kongsberg and St. Prejet anthophyllites. Correspondingly, its spectrum is more complex. Separate doublets can be distinguished by eye, but they are not so well resolved. The inner ($M4$) absorption is still the most intense, but the difference is less marked.

Bancroft *et al.* (1966) fitted a lower resolution spectrum (200 channels) of this specimen to two doublets. In this study, three doublets were needed to give an acceptable residual. At 80 K a doublet for Fe^{3+} could also be fitted (Fig. 2c). Fe^{3+} is expected to be confined to the $M2$ site in anthophyllite (Whittaker, 1960, 1971; cf. Hawthorne, 1983b). The linewidth is high for iron at a single site; but the quantity of ferric iron estimated agrees reasonably well with the analysis figure. Line broadening in this situation has been discussed by Hawthorne (1983a).

Results—low-aluminium gedrites

With the introduction in the gedrite structure of aluminium and, with it, Fe^{3+} the spectra become more complex; this trend is already apparent in the spectrum of the Bancroft anthophyllite. Results of fitting are summarized in Table 3. Residuals in fitting these spectra are generally acceptable though higher than for anthophyllites, in more highly constrained fits. A third Fe^{2+} doublet is consistently required in fitting, and as would be expected Fe^{3+} also has to be taken into account.

Bamle gedrite (001). This is the first in which separate peak maxima cannot be seen by eye. The spectrum was fitted to three Fe^{2+} doublets and one Fe^{3+}. Different spectra gave consistent fits for the Fe^{2+} doublets but not for the Fe^{3+} doublet, the estimated width of the latter in particular ranging from 0.35 (the fit cited) to 0.61 mm/sec. The F peaks are heavily masked and their estimated parameters are strongly correlated to those of the Fe^{2+} absorptions.

The inner ($M4$) absorption (doublet C) is not the most intense. It corresponds to somewhat
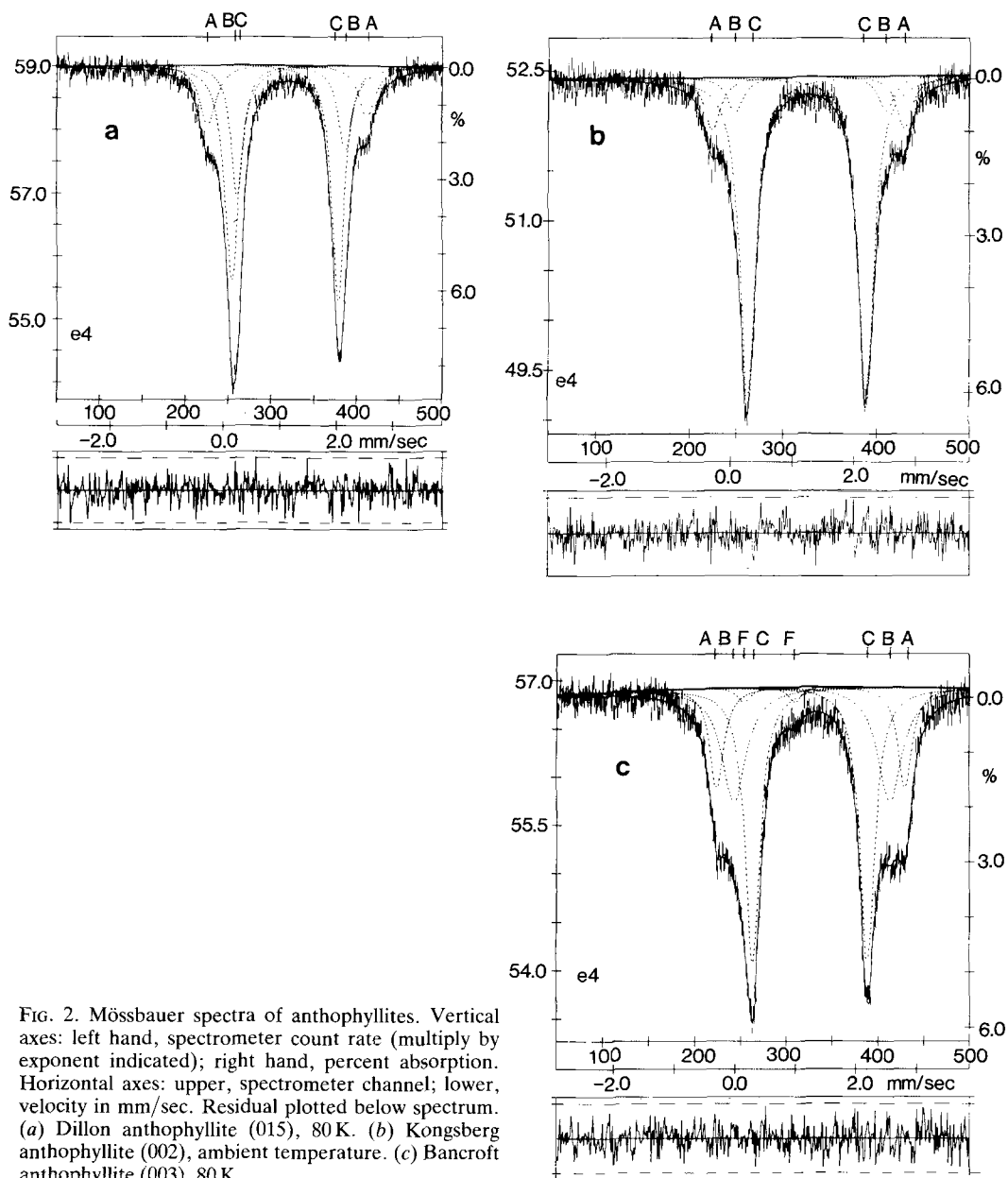
FIG. 2. Mössbauer spectra of anthophyllites. Vertical axes: left hand, spectrometer count rate (multiply by exponent indicated); right hand, percent absorption. Horizontal axes: upper, spectrometer channel; lower, velocity in mm/sec. Residual plotted below spectrum. (a) Dillon anthophyllite (015), 80 K. (b) Kongsberg anthophyllite (002), ambient temperature. (c) Bancroft anthophyllite (003), 80 K.

under half the Fe^{2+}, its relative intensity being about two-thirds that for the Bancroft anthophyllite which has a similar Fe content. The C doublet cannot represent all the $M4$ iron, and part at least of the B absorption must also arise from Fe^{2+} at $M4$.

Kalvola gedrite (004). In this spectrum (Fig. 3a), three Fe^{2+} doublets and one Fe^{3+} doublet are fitted; all the parameters are reasonable compared with other orthoamphiboles. An inflexion is visible to the low-velocity side of the higher-velocity envelope (around $+1.35$ mm/sec). This is estimated as a component of a doublet Q with a very low centre shift and quadrupole splitting.

Table 3. Mossbauer parameters for low-Al gedrites

	Temp		δ	Δ	Γ	A
001	A	A	1.128(5)	2.75(2)	0.24(3)	0.14(4)
(509)		B	1.142(8)	2.36(2)	0.35(5)	0.39(10)
		C	1.121(4)	1.92(2)	0.34(2)	0.40(5)
		F	0.53(2)	0.46(3)	0.35(4)	0.066(7)
004	A	A	1.135(2)	2.807(9)	0.28(1)	0.23(3)
(655)		B	1.146(2)	2.39(1)	0.39(3)	0.35(5)
		C	1.112(3)	1.81(1)	0.373(9)	0.35(2)
		F	0.39(2)	0.54(4)	0.49(6)	0.066(5)
		Q	1.08(2)	0.54(4)	0.19(6)	0.008(3)
008	A	A	1.138(3)	2.78(2)	0.27(2)	0.19(4)
(592)		B	1.151(2)	2.42(2)	0.37(3)	0.36(7)
		C	1.122(3)	1.86(1)	0.38(1)	0.44(2)
		Q	1.04(2)	0.53(3)	0.21(5)	0.015(3)

For notes see Table 2. Doublet asymmetries are not given:
areas of components were constrained equal for all these
fits.

Table 4. Mossbauer parameters for high-Al gedrites

	Temp		δ	Δ	Γ	A
016	A	A	1.118(2)	2.81(2)	0.31(3)	0.21(5)
(653)		B	1.116(2)	2.43(2)	0.39(4)	0.43(9)
		C	1.085(4)	1.90(2)	0.53(2)	0.33(4)
		F	0.23(2)	0.81(4)	0.29(5)	0.028(4)
016	80	A	1.268(4)	2.95(2)	0.39(1)	0.36(2)
(583)		B	1.251(4)	2.54(2)	same	0.37(2)
		C	1.205(2)	2.09(2)	same	0.22(2)
		F	0.56(4)	0.41(5)	same	0.046(6)
017	A	A	1.148(4)	2.74(2)	0.25(3)	0.14(4)
(654)		B	1.161(4)	2.39(2)	0.35(3)	0.41(7)
		C	1.126(7)	1.93(20	0.37(1)	0.33(3)
		F	0.26(5)	0.35(18)	0.72(11)	0.12(1)
009	A	A	1.170(2)	2.573(8)	0.398(9)	0.70(2)
(258)		C	1.16(1)	1.90(3)	0.44(4)	0.19(2)
		F	0.33(3)	0.39(6)	0.49(7)	0.103(8)

Notes

For notes see Table 2. Doublet asymmetries are not given:
areas of components were constrained equal except for 001,
008 where asymmetry was within area estimated error.
'same' under linewidth indicates that linewidths of doublets
were constrained equal.

009: 256 channel spectrum
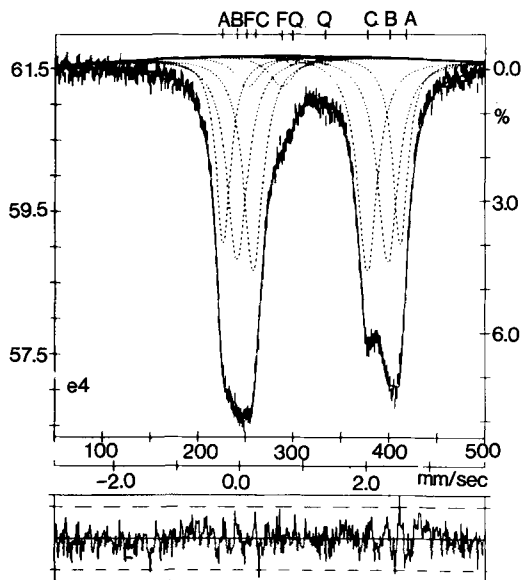
FIG. 3. Mössbauer spectra of Kalvola (low-Al) gedrite
(004), ambient temperature, as Fig. 2.

Spectra were very difficult to fit, fits tending to
diverge and requiring careful specification of
starting values.

Bullsbrook gedrite (008). The spectrum of this
gedrite is similar to that of the Kalvola gedrite.
The anomalous doublet Q again appears in the
fit, its parameters being similar to those found
for gedrite 004.

Results—high-aluminium gedrites

Results for high-aluminium gedrites are given
in Table 4. As anticipated by Seifert (1977), fitting
of the spectra does present serious problems;
these are not insurmountable, but the results must
be interpreted with caution.

Orange area gedrite I341 (016). The spectrum
of this gedrite (Fig. 4a) typifies the high-alumi-
nium gedrites. Seifert (1977) also reported a spec-
trum of this specimen but without any attempt
at fitting.

The spectrum is fitted to three Fe^{2+} doublets
and one Fe^{3+} doublet. Doublet C is not the most
intense though the structure refinement by Papike
and Ross (1970, no. 2) indicated that over half
the Fe^{2+} is at $M4$. The linewidth of the Fe^{3+} doub-
let is very high; the relative intensity of the peak
is in only moderate agreement with the amount
of Fe estimated by Papike and Ross (1970) to
be at $M2$. The residual of this fit is high, but no
better (using the word advisedly) fit could be
obtained.

A spectrum determined at 80 K was fitted to
the same combination of peaks. In this fit, all line-
widths were constrained to be equal: the residual
is acceptable, but the simplification of the model
by use of constraints results in relative peak areas
which are not in agreement with the ambient tem-
perature determination.

Orange area gedrite I34JX (017). The spectrum
of this gedrite is broadly similar to that of 016,
and shows the same complexity. It was fitted to
a similar model.
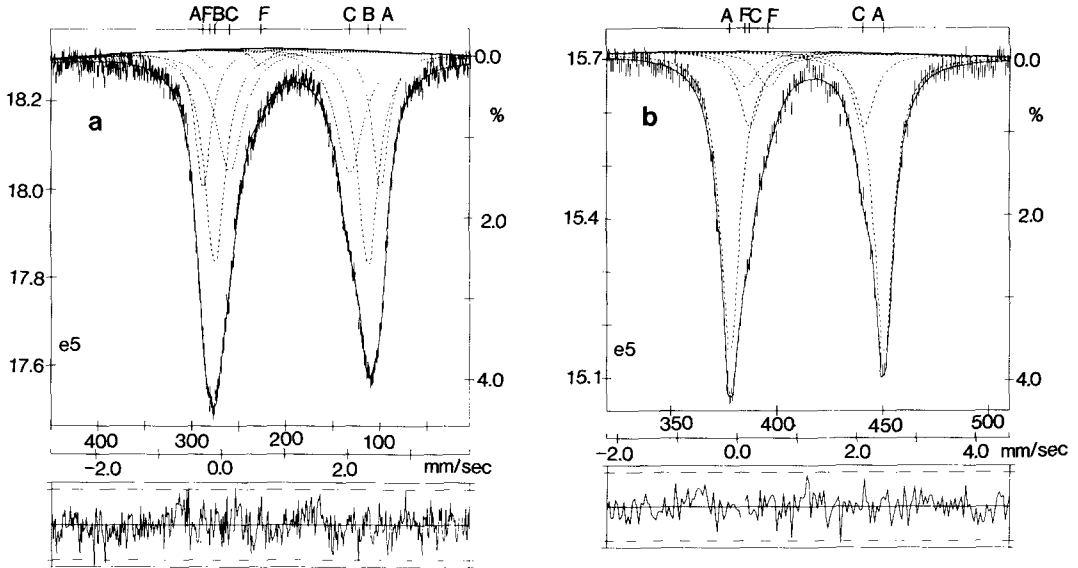
FIG. 4. Mössbauer spectra of high-Al gedrites, as Fig. 2. (*a*) Orange area gedrite I34I (016), 80 K. (*b*) Kitakami ferrogedrite (009), ambient temperature.

Kitakami ferrogedrite (009). This gedrite is of an extreme composition and must have Fe^{2+} dominant at all sites except *M2* (Al). Its spectrum (Fig. 4*b*) reverses the pattern of Mg-anthophyllites, with an outer more intense absorption and shoulders to the inside. Two doublets are fitted. The CS and QS of doublet C are low in comparison to other spectra. This absorption cannot represent all the iron at *M4*: its area is only a little over half what might be expected by allocating Al to *M2* (*M2* sites are presumably occupied almost entirely by Al), and Fe^{2+} first to *M1* + *M3* and then to *M4*. Conversely the relative area of doublet A corresponds to more than 3 Fe per formula unit: there must be some contribution to this absorption by Fe at *M4*, but splitting of the *M4* absorption by different adjacent *M2* occupancies cannot be invoked to explain why almost half of the anticipated *M4* absorption is 'borrowed' by the other doublet.

The composition of this specimen makes it of considerable potential value in understanding the Mössbauer spectra of gedrites and further work is intended.

Discussion

Mössbauer parameters. In agreement with the results of Seifert (1977) for the anthophyllites, this wider sample set shows no correlation of doublet CS with composition but correlation of QS values

and linewidths with composition can be demonstrated. For comparison with Seifert (1977), total Al is used as the compositional parameter in diagrams. Data from Seifert (1977) are included.

Of the values for Δ_A in anthophyllites (Fig. 5*a*) only that for 002 falls on the trend established by Seifert (1977), even allowing for the different analysis figures used for two of the specimens. Further work is needed to confirm this trend. Δ_C increases with increasing Al, as observed by Seifert (1977), and this trend is continued through gedrites (Fig. 5*b*). There are insufficient data points to establish a definite trend for Δ_B, but it may be increasing quite sharply with increasing Al. The QS of the outer doublet (assigned as A) in the spectrum of the ferrogedrite 009 lies on the trend suggested for doublet B in Fig. 5*b*. This trend extrapolates to meet Δ_C at anthophyllite composition.

In silicates, doublet QS decreases as site distortion increases. Site distortion is not a clearly defined concept, but is related in pyriboles to chain rotation. Rotation brings the oxygen atoms of the chain closer to a close packed configuration, and the *M* polyhedra closer to holosymmetric octahedra (Law and Whittaker, 1981; see also Hawthorne, 1983*a*). The extent of chain rotation is higher in gedrite than anthophyllite (Table 5), and this implies more symmetric polyhedra and hence higher QS.

However, from anthophyllite to gedrite the dis-
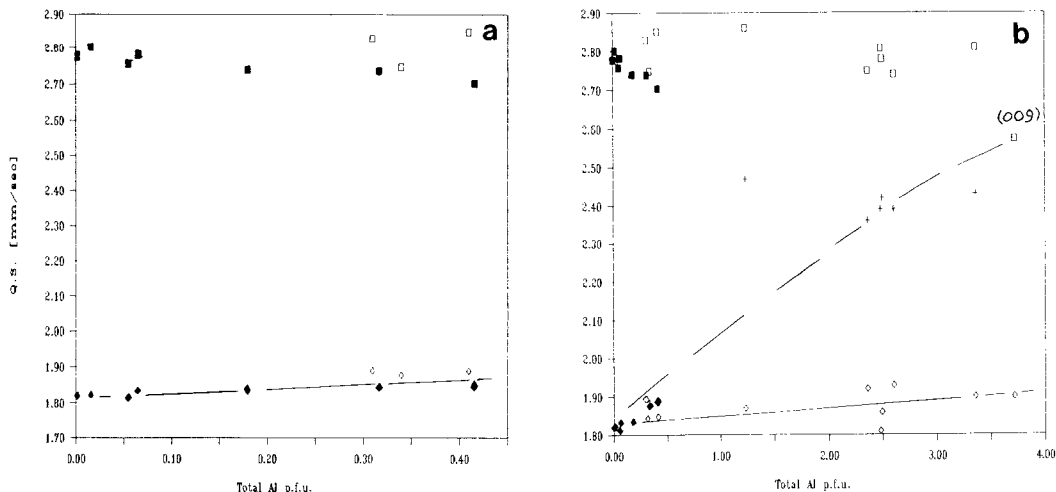
FIG. 5. Plots of QS (mm/sec) versus total aluminium. Filled symbols, data from Seifert (1977); open symbols, data from the present study. (a) Δ_A and Δ_C for anthophyllites (omitting anthophyllite 003). (b) Δ_A, Δ_B and Δ_C for all specimens.

tinction between A and B silicate chains, as measured by the chain rotation angles, also increases: see Table 5. This difference must affect, and probably will act to increase, the site distortion. These and other factors will contribute to the trends in QS. The increase in QS of doublet C from anthophyllite to gedrite may indicate that the approach to close packing and higher site symmetry is most important in the most distorted (M4) site.

Seifert (1977) found that the linewidth of doublet A in anthophyllites increases with increasing Al, and present results plot on the same trend (Fig. 6a). Γ_A for gedrites does not conform to this trend. Fig. 6b shows that there is a discontinuity corresponding to the introduction of doublet B into the fits, following which Γ_A again increases but more slowly. In contrast, Γ_C (Fig. 6c) shows a common trend across all specimens.

Doublet B cannot be assigned unambiguously to a single-site absorption. I believe that in the fitting process it represents the program's attempt to fit a single additional doublet where multiple peaks should be used. As such it 'borrows' absorption, normally from the more intense peaks. Thus in anthophyllites, dominated by doublet C (M4), Δ_B approaches Δ_C; in gedrites, it approaches Δ_A. This doublet cannot be interpreted without reference to the other peaks in the fit.

Doublet Q has an estimated CS similar to that of Fe^{2+} in the M4 site in grunerite (Law, unpublished). The QS value is similar to that for Fe^{2+}

in square planar coordination in gillespite (Bancroft et al., 1967). Thus, while these values are anomalous they are not outside the range of values for Fe^{2+} in silicates. It would, however, be unwise to put too much weight on its estimated parameters as its low-velocity component is very heavily masked resulting in high correlation coefficients with other peaks.

Spectral complexity. There is no single model of the spectrum which appears reasonable in all cases. The only consistent distinction between the fitted peaks for Fe^{2+} in the spectra seems to be between those wholly from Fe at M4 (doublet C) and others wholly from Fe at M1, M2 and M3 (in anthophyllites) or from Fe at these sites and also at M4 (gedrites). It is not clear how to apportion the A and B absorption in gedrites between M4 and the remaining sites.

Next-nearest neighbour interactions are the most likely candidate to cause the spectral complexity, but in gedrites, the question is 'which next-nearest neighbours?' Candidates include at least the two M2 sites, the A site (partly occupied in gedrites), and the next unit cell M4 sites. Differences in occupancy of the tetrahedral sites may also have an effect.

Other crystallographic possibilities include a high density of multiple chains or exsolution lamellae, both common in orthoamphiboles. It can easily be shown (Law, D.Phil. thesis, 1976; cf. Waychunas, 1986) that small peaks in the spectrum, if not fitted, can have a disproportionate
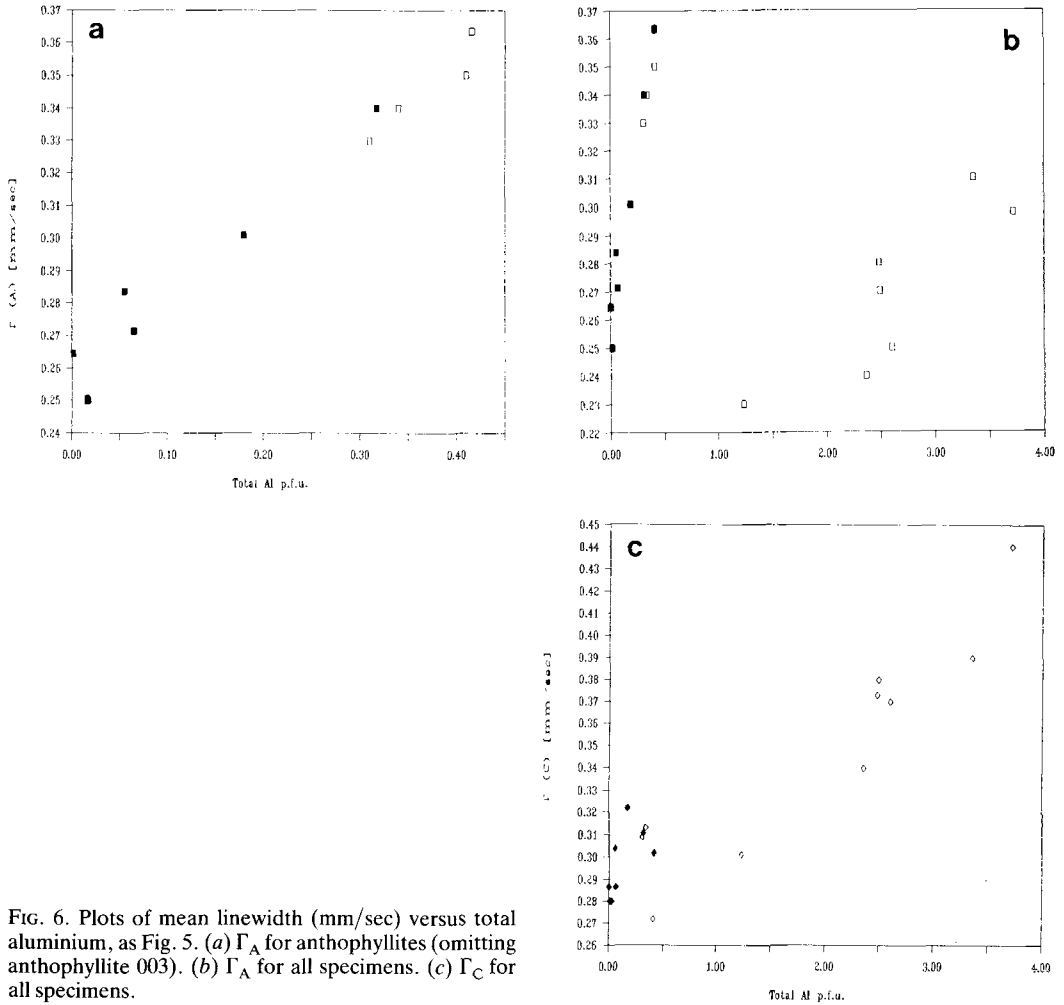
FIG. 6. Plots of mean linewidth (mm/sec) versus total aluminium, as Fig. 5. (a) Γ_A for anthophyllites (omitting anthophyllite 003). (b) Γ_A for all specimens. (c) Γ_C for all specimens.

Table 5. Chain rotation in orthoamphiboles

Amphibole	A chain	B chain	Reference
Anthophyllite 015	5.4	11.2	Finger (1969)
Gedrite 016	8.7	17.0	Papike & Ross (1970)
Gedrite (I34JX)	8.8[5]	16.2[5]	Papike & Ross (1970)
Holmquistite	6.8	8.3[5]	Irusteta & Whittaker (1975)

effect on the residual; and high residuals are found for almost all gedrite spectra. However, spectra of the Orange area gedrite 016 are among the most complex, and the detailed investigation of Papike and Ross (1970) did not identify multiple chains or exsolution. These features cannot be ruled out for all specimens of the present study,

but a consistent explanation applicable to all orthoamphiboles would seem preferable!

Williams *et al.* (1971) noted a similar effect in $C2/c$ clinopyroxenes, and also ruled out exsolution on the grounds that 'at least 25% would be required to explain' the observed or inferred multiplicity of peaks. They also ruled out lower long-

range symmetry (i.e. giving, in pyroxenes, more than two structurally distinct sites), on the basis of heavily exposed Weissenberg photographs, and concluded that there must be 'a fine domain structure ... small enough to avoid giving noticeable X-ray diffraction effects', perhaps caused by 'short range cation ordering in regions of different composition only a few unit cell dimensions across'.

We cannot avoid concluding, therefore, that the complexity of the Mössbauer spectra arises inherently from the presence of Fe species in a multiplicity of environments within single phase orthoamphiboles.

Summary

This study shows that, except at the simplest anthophyllite compositions, four peak fits do not adequately model the real Mössbauer spectra of orthoamphiboles.

Anthophyllite spectra, and those of gedrites relatively low in aluminium, can be fitted and the fits can be related to composition. High aluminium gedrites have complex spectra, but fits can be obtained albeit with high residuals. Some correlations between Mössbauer parameters and composition, as expressed by total Al, are established: anthophyllite and gedrite values lie on the same trends with the exception of Γ_C.

In spectra of high-Al gedrites the lowest QS ferrous iron absorption (normally assigned to the most distorted site, $M4$) is not the most intense even where external evidence shows that the majority of Fe^{2+} must be at $M4$. The increasing structural and compositional complexity of gedrites must lead to local as well as global differences in site geometry and to wider variation in next-nearest neighbour configurations. This is the most likely origin of the spectra's complexity, the variation in both site distortion and next-nearest neighbour configuration being significant enough to divide the absorptions to the point where the effect is more than merely an increase in estimated linewidth.

Acknowledgements

References

Bancroft, G. M., Maddock, A. G., Burns, R. G. and Strens, R. G. J. (1966) Cation distribution in anthophyllite from Mössbauer and infrared spectroscopy. *Nature* **212**, 913–5.

—— —— ——(1967) Application of the Mössbauer effect to silicate mineralogy. I: iron silicates of known crystal structure. *Geochim. Cosmochim. Acta* **31**, 2219–46.

Burns, R. G. (1972) Mixed valencies and site occupancies of iron in silicate minerals from Mössbauer spectroscopy. *Can. J. Spectroscopy* **17**, 51–9.

——and Greaves, C. (1971) Correlation of infrared and Mössbauer site population measurements of actinolites. *Am. Mineral.* **56**, 2010–33.

des Cloizeaux (1877) Sur une nouvelle anthophyllite de Bamle, en Norvège. *C.R. Acad. Sci. Paris* **84**, 1473–5.

Dollase, W. A. and Gustafson, W. I. (1982). ^{57}Fe Mössbauer spectral analysis of the sodic clinopyroxenes. *Am. Mineral.* **67**, 311–27.

Dyar, M. D. (1984) Precision and interlaboratory reproducibility of measurements of the Mössbauer effect in minerals. Ibid. **69**, 1127–44.

Eskola, P. (1936) with Kervinen, T. A paragenesis of gedrite and cummingtonite from Isopää in Kalvola, Finland. *Bull. Comm. Géol. Finlande* **115**, 475–87.

Evans, M. J. and Black, P. J. (1970) The Voigt profile of Mössbauer transmission spectra. *J. Phys. C* **3**, 2167–77.

Fabries, J. and Perseil, E. A. (1971) Nouvelles observations sur les amphiboles orthorhombiques. *Bull. Soc. fr. Mineral Crystallogr.* **94**, 385–95.

Finger, L. W. (1969) Refinement of the crystal structure of an anthophyllite. *Ann. Rep. Geophys. Lab. Washington* pp. 283.

Hawthorne, F. C. (1983a) Quantitative characterization of site occupancies in minerals. *Am. Mineral.* **68**, 287–306.

——(1983b) The crystal chemistry of the amphiboles. *Can. Mineral.* **21**, 173–480.

——(1988) Mössbauer Spectroscopy. In *'Spectroscopic methods in Mineralogy and Geology'* (Hawthorne, F. C., ed.) *Reviews in Mineralogy* **18**, 255–340.

——and Waychunas, G. A. (1988) Spectrum-fitting methods. Ibid. *Reviews in Mineralogy* **18**, 63–98.

Irusteta, M. C. and Whittaker, E. J. W. (1975) A three-dimensional refinement of the structure of holmquistite. *Acta Crystallogr.* **B31**, 145–50.

Iskyul, V. (1925) Experimental investigations in the province of the chemical composition of the silicates. See: *Mineral. Abstr.* **2**, 207.

Kendall, M. G. and Stuart, A. (1962) *Advanced theory of statistics*. London, Griffin (5th ed.).

Kunitz, W. (1930) Die Isomorphierverhaltnisse in der Hornblende-Gruppe. *Neues Jahrb. Mineral. Abh.* **60**, 171–250.

Law, A. D. (1973) Critical evaluation of statistical 'best fits' to Mössbauer spectra. *Am. Mineral.* **58**, 128–31.

——(1981) Studies of the Orthoamphiboles. II: Hydroxyl spectra of anthophyllites. *Bull. Minéral.* **104**, 423–30.

——(1982) Studies of the orthoamphiboles. III: Hydroxyl spectra of gedrites. *Mineral. Mag.* **45**, 63–71.

——and Whittaker, E. J. W. (1981) Studies of the orthoamphiboles. 1: The Mössbauer and infrared spectra of holmquistite. *Bull. Minéral.* **104**, 381–6.

Papike, J. J. and Ross, M. (1970) Gedrites: crystal structures and intracrystalline cation distributions. *Am. Mineral.* **55**, 1945–72.

Pisani, F. (1877) Description de plusieurs minéraux. *C.R. Acad. Sci. Paris* **84**, 1509–12.

Rabbit, J. C. (1948) A new study of the anthophyllite series. *Am. Mineral.* **33**, 263–323.

Robinson, P. and Jaffe, H. W. (1969) Aluminous enclaves in gedrite–cordierite gneiss from Southwestern New Hampshire. *Am. J. Sci.* **267**, 389–421.

Seifert, F. (1977) Compositional dependence of the hyperfine interaction of ^{57}Fe in anthophyllite. *Phys. Chem. Minerals* **1**, 43–52.

——and Virgo, D. (1974) Temperature dependence of intracrystalline Fe^{2+}–Mg distribution in a natural anthophyllite. *Carnegie Inst. Washington Yearb.* **73**, 405–11.

Seki, Y. and Yamasaki, M. (1957) Aluminian ferro-anthophyllite from the Kitakami mountainland, northeastern Japan. *Am. Mineral.* **42**, 506–20.

Simpson, E. S. (1931) Contributions to the mineralogy of Western Australia. Series VI. *J. Royal Soc. West. Austral.* **17**, 137–49.

Spear, F. S. (1980) The gedrite–anthophyllite solvus and the composition limits of orthoamphibole from the Post Pond Volcanics, Vermont. *Am. Mineral.* **65**, 1103–18.

Squires, G. L. (1968) *Practical Physics.* McGraw-Hill.

Stevens, J. G. and Preston, R. S. (1970) Useful information for ^{57}Fe Mössbauer spectroscopy. In *Mössbauer effect Data Index, Appendix G*, 16.

Stone, A. J. (1967) Least Squares fitting of Mössbauer spectra. Appendix to Bancroft, G. M., Maddock, A. G., Ong, W. K., Prince, R. H. and Stone, A. J., Mössbauer Spectra of Iron(III) diketone complexes. *J. Chem. Soc. A*, 1971.

Tilley, C. E. (1957) Paragenisis of anthophyllite and hornblende from the Bancroft area, Ontario. *Am. Mineral.* **42**, 412–16.

Waychunas, G. A. (1986) Performance and use of Mössbauer goodness-of-fit parameters: response to spectra of varying signal/noise ratio and possible misinterpretations. Ibid. **71**, 1261–5.

Whittaker, E. J. W. (1960) The crystal chemistry of the amphiboles. *Acta Crystallogr.* **13**, 291–8.

——(1971) Madelung energies and site preferences in amphiboles I. *Am. Mineral.* **56**, 980–96.

Williams, P. G. L., Bancroft, G. M., Brown, M. G. and Turnock, A. C. (1971) Anomalous Mössbauer spectra of C2/c clinopyroxenes. *Nature Phys. Sci.* **230**, 149–51.

Appendix: Propagation of estimated errors

Use of the dispersion (variance–covariance) matrix to ensure correct estimated errors are assigned to calculated Mössbauer parameters is discussed by Hawthorne and Waychunas (1988). The variance of a function $y = f(x_1, x_2, \ldots, x_n)$ of a set of experimental results can be written as

$$\sigma_y^2 = \Sigma_i \Sigma_j \left[\sigma_{ij}^2 \frac{\partial f}{\partial x_i} \frac{\partial f}{\partial x_j} \right]$$

where σ_{ij}^2 is the covariance of x_i with x_j and for consistency σ_{ii}^2 denotes the variance of x_i. A more detailed derivation can be found in Kendall and Stuart (1962, p. 232).

Conversion of raw fitted Mössbauer parameters to their final form involves arithmetic calculations for which the corresponding error propagation functions can be concisely stated in forms following Squires (1968):

for linear combination, $f(x) = \Sigma_i a_i x_i$,

$$\sigma_y^2 = \Sigma_i \Sigma_j a_i a_j \sigma_{ij}^2;$$

for product, $f(x) = x_i \cdot x_j$, and for quotient, $f(x) = x_i/x_j$;

$$\sigma_y^2 = \frac{\sigma_{ii}^2}{x_i^2} + \frac{\sigma_{jj}^2}{x_j^2} \pm 2\frac{\sigma_{ij}^2}{x_i x_j},$$

where the final sign is + for product and − for quotient.

Correlation coefficients, which give an estimate of the interdependence of the several fitted parameters in the fitting process, are derived from the variance–covariance matrix. The correlation coefficient C_{ij} is:

$$C_{ij} = \frac{\sigma_{ij}^2}{\sqrt{(\sigma_{ii}^2 \sigma_{jj}^2)}}.$$